



**HAL**  
open science

# Planar Wideband Microstrip Antenna with Inclined Radiation Pattern for C-Band Airborne Applications

Sofiene Bouaziz, Ahmed Ali Mohamed Ali, Sami Hebib, Hervé Aubert

► **To cite this version:**

Sofiene Bouaziz, Ahmed Ali Mohamed Ali, Sami Hebib, Hervé Aubert. Planar Wideband Microstrip Antenna with Inclined Radiation Pattern for C-Band Airborne Applications. The 4th European Conference on Antennas and Propagation (EuCAP), Apr 2010, Barcelone, Spain. pp. 1-4. hal-00465058

**HAL Id: hal-00465058**

**<https://hal.science/hal-00465058>**

Submitted on 18 Mar 2010

**HAL** is a multi-disciplinary open access archive for the deposit and dissemination of scientific research documents, whether they are published or not. The documents may come from teaching and research institutions in France or abroad, or from public or private research centers.

L'archive ouverte pluridisciplinaire **HAL**, est destinée au dépôt et à la diffusion de documents scientifiques de niveau recherche, publiés ou non, émanant des établissements d'enseignement et de recherche français ou étrangers, des laboratoires publics ou privés.

# Planar Wideband Microstrip Antenna with Inclined Radiation Pattern for C-Band Airborne Applications

Sofiène Bouaziz<sup>1</sup>, Ahmed Ali<sup>2</sup>, Sami Hebib<sup>3</sup> and Hervé Aubert<sup>4</sup>  
 CNRS ; LAAS ; 7 avenue du colonel Roche, F-31077 Toulouse, France  
 Université de Toulouse ; UPS, INSA, INP, ISAE ; LAAS ; F-31077 Toulouse, France  
 7 avenue colonel Roche avenue, F-31077 Toulouse, France

<sup>1</sup>sbouaziz@laas.fr

<sup>2</sup>aali@laas.fr

<sup>3</sup>hebib@laas.fr

<sup>4</sup>haubert@laas.fr

**Abstract**—This paper presents the design and experimental validation of an original single layer planar wideband microstrip antenna for C-band airborne applications. This antenna printed on a 787 $\mu\text{m}$ -thick substrate exhibits wideband performance and inclined radiation patterns. The measured results are in good agreement with the simulated ones in terms of bandwidth (more than 15% impedance bandwidth at 7.1GHz) and radiation pattern requirements.

## I. INTRODUCTION

In applications where low cost, light weight, conformability and ease of fabrication are major design constraints, microstrip antennas are excellent candidates. In addition, radiation pattern shape controlling is one of the key advantages of these antennas. In fact, various practical methods have been devoted for this purpose, e.g. the modified finite ground plane microstrip patch antenna [1] and the printed Yagi array antenna [2]. However, the most important drawback of microstrip antennas is its narrow bandwidth. Several broadbanding techniques have been proposed in order to overcome this disadvantage, namely the E-shaped slot-loaded patch antenna [3] and the use of electromagnetically-coupled parasitic patches either in coplanar [4] or stacked topologies [5, 6].

This paper deals with the design and experimental validation of an original single layer quarter-wave patch antenna with coplanar quarter-wave parasitic elements and planar dual microstrip line feed for airborne C-band applications. Besides its low thickness (787 $\mu\text{m}$ ), the designed antenna presents good performance in terms of wide bandwidth behaviour and unidirectional, low-frequency dependent, inclined radiation patterns. Section II provides the antenna design and principles of operation. The simulation and experimental results are shown and discussed in section III. Finally, conclusion and perspectives are given in section IV.

## II. ANTENNA DESIGN AND PRINCIPLES OF OPERATION

The antenna presented in this paper will be affixed on the upper side of the plane wings. It's used to achieve radio-frequency wireless communication of measured pressure data. These data are collected over different locations on the two plane wings (therefore different antennas with separate frequency bands are needed) and then received by another

appropriate antenna located inside the cabin (see Fig.1). Consequently, on the one hand, the designed antenna needs to be mechanically robust with small-height dimensions (less than 1mm).

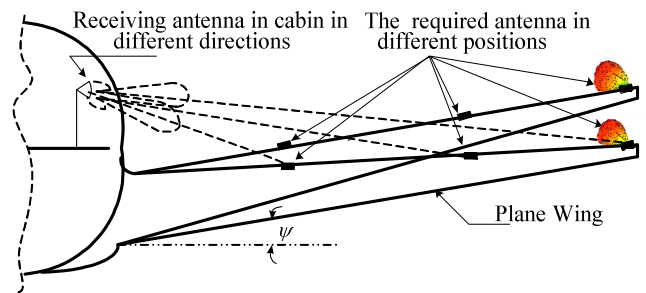


Fig.1 Schematic layout showing the geometrical setup of the required antenna on the plane wing together with the receiving antenna inside the cabin.

On the other hand, by taking into account the change of the inclination angle  $\psi$  of the wing (Fig. 1) with respect to the horizontal direction (typical values vary from  $+5^\circ$  at rest to  $+15^\circ$  during the flight), the antenna is required to have a sufficiently “flat” radiation pattern to optimize the polarization mismatch losses.

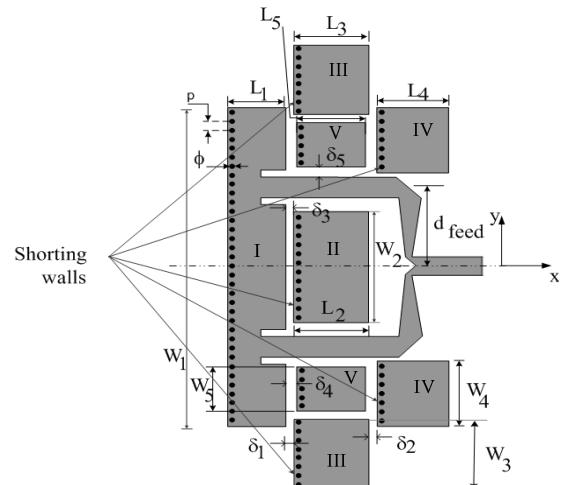


Fig. 2 Geometry of the designed quarter-wave antenna with coplanar quarter-wave parasitic patches

TABLE I  
DIMENSIONS IN MM OF THE FINAL DESIGNED ANTENNA

$L_1$	$L_2$	$L_3$	$L_4$	$L_5$	$W_1$	$W_2$	$W_3$	$W_4$	$W_5$	$\delta_1$	$\delta_2$	$\delta_3$	$\delta_4$	$\delta_5$	$d_{\text{feed}}$
6.57	8.15	7.40	6.85	7.40	40	16	8	8	7.1	0.2	0.4	1.2	0.3	0.85	10

The designed 787 $\mu\text{m}$ -thick microstrip antenna is displayed in Fig.2. The antenna structure, endowed with a dual microstrip feed, consists of a quarter-wave driven patch (marked with “I” in Fig.2) coupled to additional coplanar parasitic quarter-wave patches (marked with “II”, “III”, “IV” and “V” in Fig.2). To increase the antenna directivity, the antenna width is doubled and a simple microstrip corporate feed network with tapered impedance transformer lines is used for excitation. The parasitic quarter-wave patches were printed on the occupied area by the feed network for miniaturization purposes. The electromagnetic coupling between the parasitic patches and the driven patch allows wideband performance and higher directivity levels. The presence of the shorting walls located on the driven patch helps to create asymmetrical current distribution. The inclined radiation patterns are then obtained by placing adequately the quarter-wave parasitic patches with respect to the driven patch. The dimensions of the final antenna are summarized in table I. The effects of varying these dimensions were previously discussed by the authors in [7].

### III. SIMULATION AND EXPERIMENTAL RESULTS

The antenna electromagnetic simulations have been carried out using MoM-based Zeland IE3D simulator. The antenna structure is printed on a 0.787mm-thick substrate (Neltec NY9217) with  $\epsilon_r = 2.17$  and  $\tan\delta = 8.10^{-4}$ . The fabricated antenna is shown in Fig.3. The overall size of the antenna presented in this Figure is 40mm x 60mm. The shorting walls were created with the means of metalized via-holes with 1mm diameter and 1.5mm pitch. For better performance of the radiating patches, their resonant lengths have been corrected according to the equations of [8].

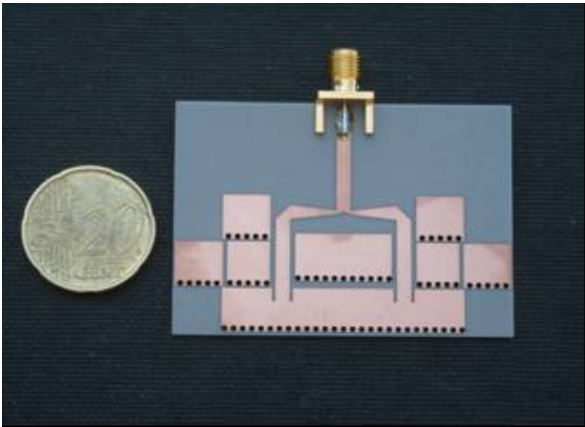


Fig.3 The fabricated antenna on a Neltec NY9217 substrate.

The S-parameter measurement of the fabricated antenna was performed with Anritsu 37397D VNA. Fig. 4 displays the

antenna simulated  $|S_{11}|$  compared to the measured one. A 13% shift is observed between the simulated minimum  $|S_{11}|$  (7.5 GHz) and measured minimum  $|S_{11}|$  (7.4 GHz). This frequency shift can be explained by the inaccuracy of fabrication of the via-holes and the finite ground plane dimension.

Both in simulation and measurement, the designed antenna provides a 15% impedance bandwidth ( $|S_{11}| < -10$  dB).

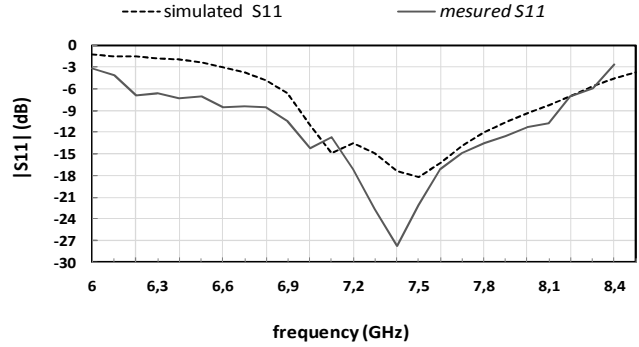


Fig.4 Simulated and measured  $|S_{11}|$  of the designed antenna

Fig. 5 plots the antenna simulated maximum gain curve versus frequencies within the antenna's bandwidth. This gain curve exhibits a maximum value of 6.5 dBi at 7.1 GHz and a minimum value of 5 dBi at 7.3 GHz.

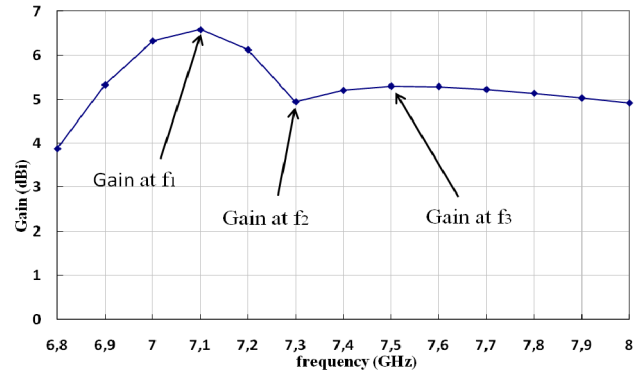


Fig.5 Simulated maximum gain versus frequency

Fig.6 illustrates the surface electric current distribution at  $f_1=7.1\text{GHz}$ ,  $f_2=7.3\text{GHz}$  and  $f_3=7.5\text{GHz}$  (See marked frequencies in Fig.5). It explains the variation of the maximum gain curve previously depicted in Fig.5. At 7.1GHz and 7.5GHz, the current density distribution on the patches marked with “III” and “V” in fig.2 is in-phase and a higher magnitude (illustrated respectively in Fig.6 (a) and Fig.6 (c)). In fig.6 (a), i.e., at 7.1GHz, current density distribution presents highest vector magnitude. In this case, the antenna gain value reaches a maximum (more than 6 dBi simulated maximum gain value at 7.1GHz).

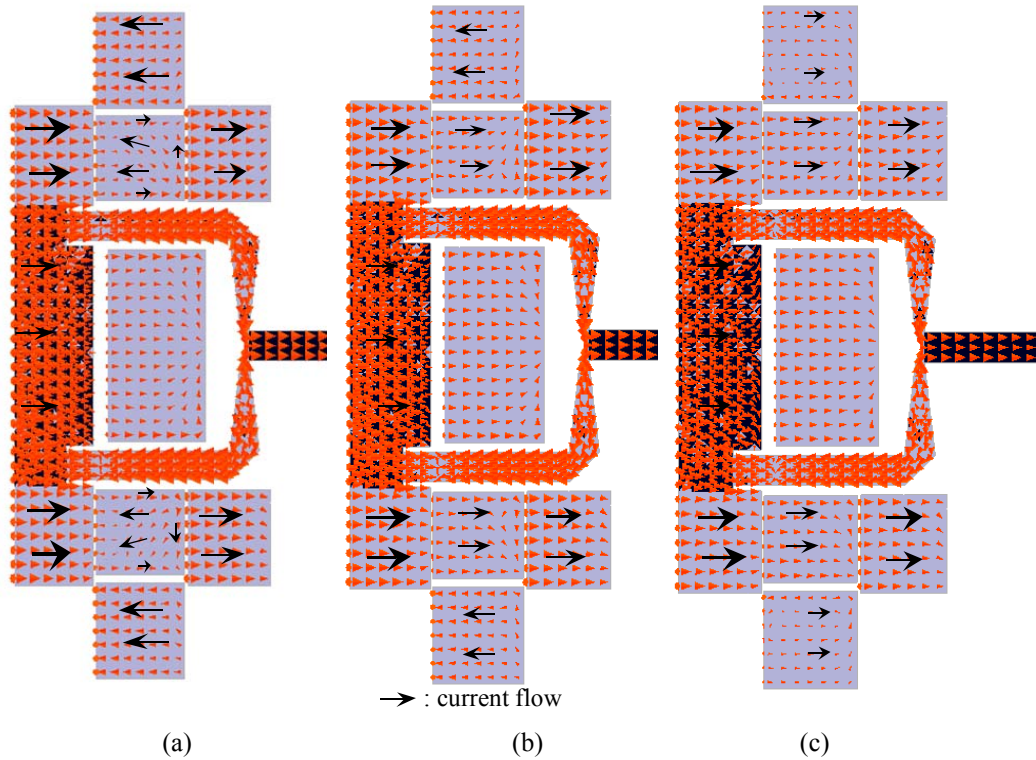


Fig. 6 The surface electric current density distribution at (a) 7.1GHz, (b) 7.3GHz and (c) 7.5GHz.

In contrast, the antenna gain value reaches a minimum (lower than 5dBi at 7.3 GHz) when the current density distribution on the two parasitic patches marked with “III” is anti-phase with the current density distribution on the patches marked with “V” (Fig.6 (b)). Fig.7 shows the simulated and measured radiation patterns of the designed antenna in the E-plane at different frequencies (6.9 GHz, 7.2 GHz and 7.6 GHz). Radiation pattern measurement has been performed in the LAAS-CNRS anechoic chamber. More than 5 dBi measured gain values are obtained at both 7.2 GHz and 7.6 GHz. The

noise brought by anechoic chamber, cables and measurement instruments provide a small difference in the gain values between measured and simulated results. Due to the SMA connector and the feeding cable of the antenna, an undesirable minor lobe is observed in the radiation pattern shown in fig.6 (b). Finally, the inclined radiation requirements are clearly validated experimentally: the designed antenna has inclined radiation patterns with measured gain values of 5 dBi at 45° elevation angle that would be point at the receiving antenna inside the plane cabin.

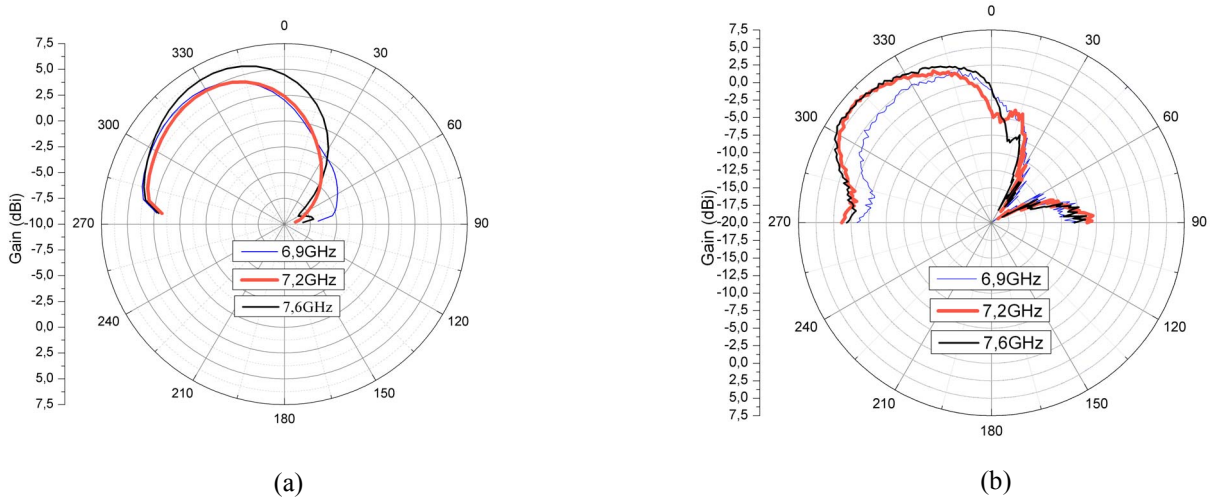


Fig.7 (a) Simulated and (b) measured radiation patterns of the designed antenna in the E-plane at different frequencies.

#### IV. CONCLUSION

This paper presented the design and measurement of a single-layer low profile wideband microstrip antenna printed on 787 $\mu\text{m}$  thick substrate. The simulated and measured results were shown and discussed. More than 15% impedance bandwidth at 7.1 GHz is obtained and the inclined radiation patterns are experimentally validated. Future work will focus on the bandwidth characterization in terms of bit error rate for appropriate modulation schemes to verify the designed antenna for the foreseen application.

#### ACKNOWLEDGMENT

This work is supported by the Project of "Pôle de compétitivité" entitled *Systèmes Autonomes Communicants En Réseau* (SACER).

#### REFERENCES

- [1] T. Namiki, Y. Murayama, K. Ito, "Improving radiation-pattern distortion of a patch antenna having a finite ground plane", *IEEE Trans. Antennas Propagat.*, vol. 51, no. 3, pp. 478-482, 2003.
- [2] J. Huang, "Planar microstrip Yagi array antenna", *Antennas and Propagation Society International Symposium, AP-S. Digest*, vol. 2, pp. 894-897, 1989.
- [3] F. Yang, X. Zhang, X. Ye and R. Samii, "Wide-band E-shaped patch antennas for wireless communications", *IEEE Trans. Antennas Propagat.*, vol. 49, no. 7, pp. 1094-1100, July, 2001.
- [4] L. Peng, C. Ruan and Y. Zhang, "A novel compact broadband microstrip antenna", *Asia-Pacific Microwave Conference*, Dec. 2007.
- [5] R. B. Waterhouse, "Design of probe-fed stacked patches", *IEEE Trans. Antennas and Propagat.*, vol. 47, no. 12, pp. 1780-1784, Dec., 1999.
- [6] S. D. Targonski, R. B. Waterhouse and D. M. Pozar, "Design of wide-band aperture-stacked patch microstrip antennas", *IEEE Trans. Antennas Propagat.*, vol. 46, no. 9, pp. 1245-1251, Sept., 1998.
- [7] S. Bouaziz, A. Ali, H. Aubert, "Low-Profile Wideband Antenna with Unidirectional Inclined Radiation Pattern for C-band Airborne Application", *Asia-Pacific Microwave Conference*, Dec. 2009.
- [8] M. Sanad, "Effect of the shorting posts on short circuit microstrip antennas", *IEEE/AP-S Int. Symp. Digest*, pp. 701-704, 1994.